



Research paper

Modeling and Simulation of DC Electric Railway System with Regenerative Braking: A Case Study of Isfahan Metro Line 1

P. Hamedani^{1,*}, S. S. Fazel², M. Shahbazi³

¹ Department of Railway Engineering and Transportation Planning, University of Isfahan, Isfahan, Iran.

² School of Railway Engineering, Iran University of Science and Technology, Tehran, Iran.

³ Department of Engineering, Durham University, Durham, U.K.

Article Info

Article History:

Received 13 February 2024

Reviewed 15 March 2024

Revised 05 April 2024

Accepted 29 April 2024

Keywords:

DC electric railway

Regenerative braking

Power flow

Traction power systems

Isfahan metro

Train movement simulation

*Corresponding Author's Email Address:

p.hamedani@eng.ui.ac.ir

Abstract

Background and Objectives: Modeling and simulation of electric railway networks is an important issue due to their non-linear and variant nature. This problem becomes more serious with the enormous growth in public transportation tracks and the number of moving trains. Therefore, the main aim of this paper is to present a simple and applicable simulation method for DC electric railway systems.

Methods: A train movement simulator in a DC electric railway line is developed using Matlab software. A case study based on the practical parameters of Isfahan Metro Line 1 is performed. The simulator includes the train mechanical movement model and power supply system model. Regenerative braking and driving control modes with coasting control are applied in the simulation.

Results: The simulation results of the power network are presented for a single train traveling in both up and down directions. Results manifest the correctness and simplicity of the suggested method which facilitates the investigation of the DC electric railway networks.

Conclusion: According to the results, the train current is consistent with the electric power demand of the train. But the pantograph voltage has an opposite relationship with its electric power demand. In braking times, the excess power of the train is injected into the electrical network, and thus, overvoltage and undervoltage occur in the overhead contact line and the substation busbar. Therefore, at the maximum braking power of the train, the pantograph voltage reaches its maximum. The highest amount of fluctuation is related to the substation that is closest to the train. As the train moves away from the traction substations, the voltage fluctuations decrease and vice versa.

This work is distributed under the CC BY license (<http://creativecommons.org/licenses/by/4.0/>)



Introduction

In recent years, with the increase in population, the need to expand the public transportation network has increased. One of the most popular methods of urban transportation is using the urban metro system. Urban metro systems are usually fed through DC power supply systems. Two common electrification methods for metro trains are the third rail system and overhead contact

system (OCS). The third rail system is usually used at the standard voltage level of 750 V. To increase the speed and capacity of the transportation network, the overhead contact network with 1500 VDC and 3000 VDC is utilized [1]-[4].

To design, and analyze the performance of traction stations and electric train electrification systems, as well as the technical-economic justification of electric rail projects, electrical modeling and simulation of the rail

power supply network is necessary [1]-[4]. In addition, the electrical simulation of the railway power supply network requires the extraction of movement graphs and speed profiles of trains. Determining the movement graphs and speed profile of trains can be very useful in calculating the train performance, determining the train travel time, the planning of train movement, increasing the line capacity, and also determining the amount of energy consumption [5]-[7]. So far, several studies have been conducted in the field of train movement simulation and movement profile extraction. Modeling the movement of a train on a track depends on several factors, and therefore the extraction of movement graphs requires complex analytical methods [5]. Train and track parameters such as train weight, aerodynamic resistance force, quality of brakes, gradient profile and curve profile of the movement path, friction coefficient, as well as speed and acceleration limitations, are among the factors that are effective in modeling the train movement. In [5], the main equations required for train movement calculations are presented. In [8]-[13], the speed profile of the trains has been optimized in the electric railway track to reduce energy consumption. The results were repeated on different railway lines and showed a reduction in travel time and energy consumption.

The electric railway network has a time-varying nonlinear model. But in general, the model of the DC railway network is simpler than the AC railway network. The DC electric railway network modeling has been studied in the literature [14]-[23]. Gauss-Seidel and Newton-Raphson are common methods in solving DC railway power flow [17]-[19]. In addition, the current injection method, point-Jacobi method, Zollenkopf's bifactorisation, and incomplete Cholesky conjugate gradient method, have been proposed and investigated [20]-[23]. Recently, the application of electric trains with regenerative braking has been significantly expanded in the urban transport network and subways. Various studies have been reported on the evaluation and management of electric energy consumption in electric railway networks, including regenerative trains [9], [19], [24]-[30]. However, consideration of the regenerative braking capability complicates the railway network modeling and the power flow solving.

This paper proposes a simplified simulation model for the DC electric railway network including the train mechanical movement model and power supply system model. Regenerative braking and driving control modes with coasting control are applied in the simulation. Based on the route data of Isfahan Metro Line 1, the simulation results of the power network are presented for a train traveling in both up and down directions. Results manifest the correctness and simplicity of the suggested method which facilitates the investigation of the DC electric railway networks.

Modeling of DC Electric Railway

A. Train Kinematics Modeling

For kinematics modeling of the trains, Newton's second law of motion can be utilized. The main equation of movement can be expressed as [31]:

$$F_T = TE - F_{grad} - F_{drag} = M_{eff}\alpha \tag{1}$$

where F_T is the total force [N]. TE , F_{grad} , and F_{drag} represent the traction effort [N], the gradient force [N], and the drag resistance force [N], respectively. The curvature resistance force is neglected in this paper. α is the acceleration of the train [m/s^2]. Moreover, M_{eff} is the effective mass of the train [Kg] and can be written as:

$$M_{eff} = (1+\lambda) M_t + M_l \tag{2}$$

M_t and M_l are the tare mass and payload mass of the train [Kg], respectively. Furthermore, λ is the rotary allowance. The drag resistance force can be calculated according to the Davis equation:

$$F_{drag} = a + bV + cV^2 \tag{3}$$

where F_{drag} represents the drag resistance force [N]. a [N], b [Nh/Km], and c [Nh²/Km²] are the Davis coefficients. V is the train speed [Km/h]. The gradient force can be written as:

$$F_{grad} = M g \sin(\theta) \tag{4}$$

in which g (9.81 m/s^2) and θ [rad] are the gravity acceleration and the slope angle, respectively. $M=M_t+M_l$ [Kg] is the train mass.

As shown in Fig. 1, to model the train movement, four different operating modes can be considered including traction, cruising, coasting, and braking modes [31].

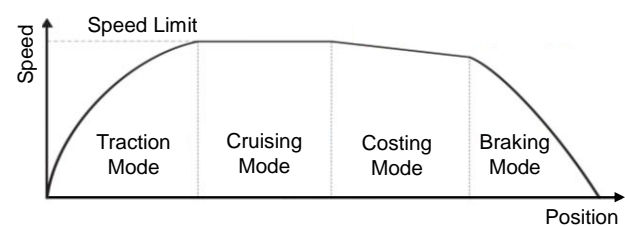


Fig. 1: Train operating modes.

The traction mode is the region in which the train accelerates. The cruising mode is the region in which the train runs at maximum speed according to the speed limits. The coasting mode is the region in which the train runs with zero tractive effort in a downhill. The braking mode is the region in which the train decelerates.

In each operating mode, by solving the train movement specified in (1), the train position, speed, and acceleration can be extracted, as shown in Table 1. The tractive effort (TE) is the generated force by the traction motors for overcoming the resistance forces imposed to

the running train on the route. In the braking mode, the braking force (BR) is the generated by the braking system for stopping the train. Fig. 2 presents the typical tractive effort [KN] and braking force [KN] curves versus the speed [Km/h].

Table 1: Train Movement Equation in Different Modes

Operating Modes	Equations
Traction	$TE > Mg \sin(\theta) + F_{drag}$
	$\alpha = \frac{TE - Mg \sin(\theta) - F_{drag}}{M_{eff}}$
Cruising	$TE = Mg \sin(\theta) + F_{drag}$
	$\alpha = 0$
Costing	$TE = 0$
	$\alpha = \frac{-Mg \sin(\theta) - F_{drag}}{M_{eff}}$
Braking	$BR < 0$
	$\alpha = \frac{BR - Mg \sin(\theta) - F_{drag}}{M_{eff}}$

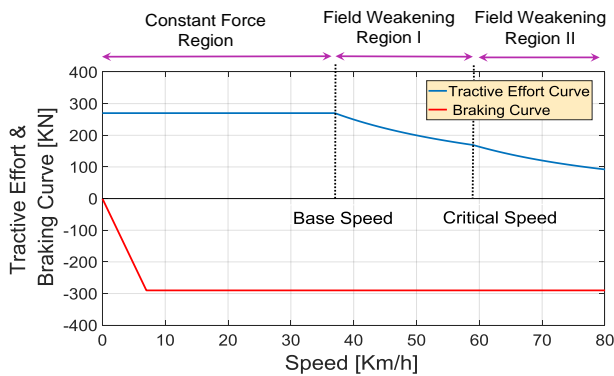


Fig. 2: Tractive effort and braking curve.

The tractive effort curve consists of three different regions including constant force region, field weakening region I, and field weakening region II.

The constant force region is the area below the base speed. The flux-weakening region I starts from the base speed (due to the power limitation) and ends at the critical speed. The flux-weakening region II is the area above the critical speed (due to the motor limitation).

B. Train Power Modeling

The next step for simulating the train movement is to calculate the required mechanical power of the train (P_{me}):

$$P_{me} = TE \times V \quad (5)$$

The required electric power of the train (P_{el}) can be extracted with respect to the motoring and braking condition of the train [31], [32]. In the motoring operating condition, the mechanical power is positive while in the braking operating condition, the mechanical power is negative.

$$P_{el} = \begin{cases} \frac{P_{me}}{\eta} & \text{if } P_{me} \geq 0 \\ P_{me} \times \eta & \text{if } P_{me} < 0 \end{cases} \quad (6)$$

where η is the efficiency of the traction system from the pantograph to the wheel. P_{me} [W] and P_{el} [W] are the mechanical and electrical power of the train, respectively. The total power demand of the train (P_{train}) is the summation of the electrical power and the auxiliary power [31], [32]:

$$P_{train} = P_{el} + P_{aux} \quad (7)$$

P_{aux} [W] represents the auxiliary power that includes lighting, air conditioning, and other energy consumptions of the passengers.

C. DC Railway Power Network Modeling

The power network includes traction substations, overhead contact lines (OCLs), rails as return current circuits (RCRs), and trains. Fig. 3 shows the structure of the DC railway power network between two traction substations. Fig. 4 illustrates the equivalent circuit of the DC railway power network between two traction substations.

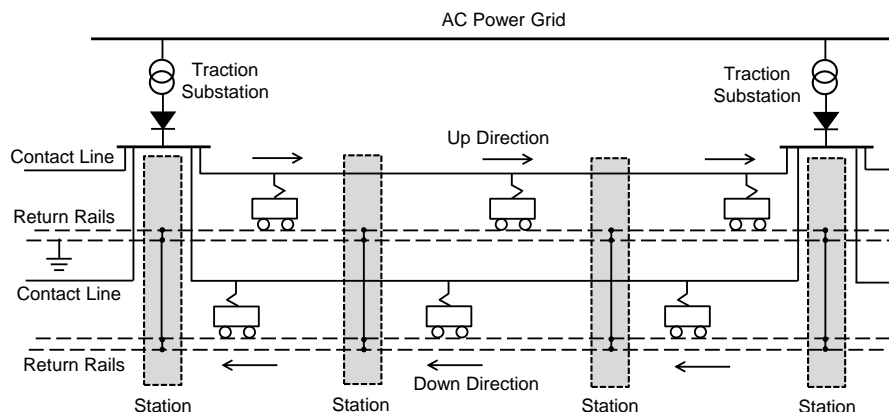


Fig. 3: Structure of the DC railway power network.

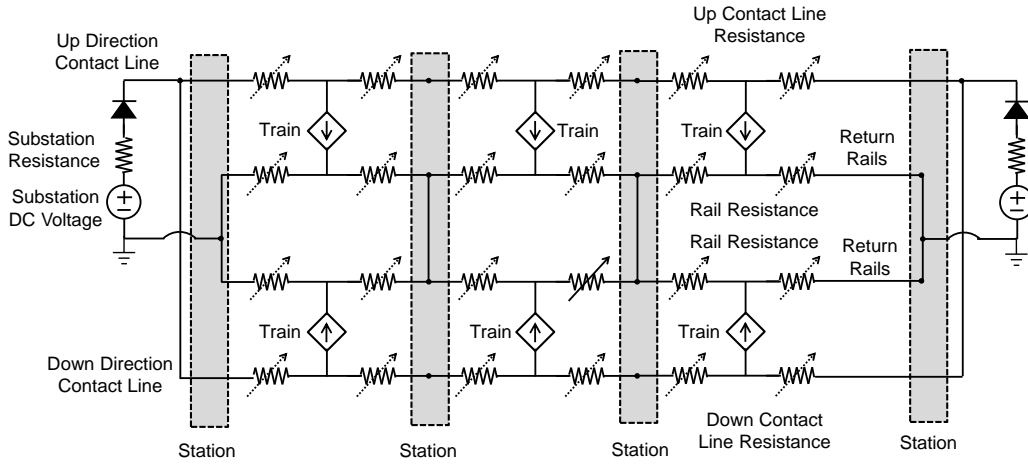


Fig. 4: Equivalent circuit of the DC railway power network between two traction substations.

In this work, the voltage regulation characteristic of the substation is assumed linear. Therefore, Thevenin’s model of the traction substation can be utilized [19]. In Isfahan Metro, twelve-pulse rectifiers are used in the substations. The no-load voltage can be considered 1588 V [32]. The rated voltage and current can be considered 1500 V and 2100 A, respectively. As a result, the Thevenin’s voltage is equal to 1500 V and the equivalent resistance of the traction substations can be calculated as:

$$R_{sub} = \frac{\Delta V}{\Delta I} = \frac{V_{no-load} - V_{rated}}{I_{rated} - 0} = 0.0419 \Omega \quad (8)$$

As shown in Fig. 4, in a DC railway power network, the OCL and RCR are modeled with resistance. The total resistance of the overhead contact line (R_c) and return current circuit between two passenger stations (R_r) can be written as:

$$R_c = L \times r_c \quad (9)$$

$$R_r = L \times \frac{r_r}{2} \quad (10)$$

where r_c [Ω/Km] and r_r [Ω/Km] are the resistance of the overhead contact line and rails per track. L is the length of the track between two consecutive passenger stations [Km]. The OCL and RCR resistance between the train and the previous passenger station depends on the length [18]:

$$R_c' = D \times r_c \quad (11)$$

$$R_r' = D \times \frac{r_r}{2} \quad (12)$$

where D is the traveled distance of the train from the previous stations [Km]. R_c' [Ω] and R_r' [Ω] are the OCL and RCR resistance between the train and the previous passenger station, respectively.

The OCL and RCR resistance between the train and the next passenger station can be expressed as [18]:

$$R_c'' = (L - D) \times r_c \quad (13)$$

$$R_r'' = (L - D) \times \frac{r_r}{2} \quad (14)$$

R_c'' [Ω] and R_r'' [Ω] are the OCL and RCR resistance between the train and the next passenger station, respectively. This method can be used for calculating the OCL and RCR resistances in both up and down tracks.

The trains are modeled as voltage-dependent current sources:

$$I_{train} = \frac{P_{train}}{V_{train}} \quad (15)$$

in which V_{train} [V] and I_{train} [A] are the pantograph voltage and current, respectively. P_{train} [W] can be calculated using (7). The direction of each current source depends on the motoring or braking condition of the train.

Results and Discussion

Based on the modeling strategy of the DC electric railway described in previous sections, a train movement simulator has been developed in this work. In this section, a case study based on the Isfahan Metro Line 1 is presented.

In Table 2, the train and line parameters required for the mechanical simulation of the rail system are represented. Line 1 of the Isfahan Metro is about 20.464 Km long. The initial design of this line had 21 passenger stations and 7 traction substations. In this work, the initial design of Line 1 is studied. In Table 3, the location of the passenger stations and traction substations of Isfahan Metro Line 1 are listed. The up track corresponds to the running direction from the GHO station to the DEMO station. The down track corresponds to the running direction from the DEMO station to the GHO station. The traction substations consist of twelve-pulse rectifiers.

Trains are fed with the OCL system. The rated voltage of the DC OCL is 1500 V.

Table 2: Train and Track Parameters of Isfahan Metro Line 1

Parameters	Value
Train Configuration	Tc-Mp-M-Mp-Tc
Train Tare Mass	176 [tons]
Passenger Mass in AW2 (6 Person/m ²)	78.19 [tons]
Max. Speed	80 [Km/h]
Base Speed	37 [Km/h]
Critical Speed	59 [Km/h]
Max. Tractive Effort	270 [kN]
Max. Braking Effort	290 [kN]
Auxiliary Power	380 [Kwatt]
Efficiency	90 [%]
Max. Acceleration	1 [m/s ²]
Max. Deceleration	1.1 [m/s ²]
Rotary Allowance	1.088
Davis Constants	a= 4226.816 b= 35.5866 c= 0.51516
Dwell Time	30 [sec]
RCR Resistance per track per Km (a Rail S49)	22.5 [mΩ/Km]
OCL Resistance per Km	55.5 [mΩ/Km]

Fig. 5 shows the gradient profile of Isfahan Metro Line 1 for the up track. According to the mechanical and dynamic equations of train movement that were introduced in section 2 and also using the route parameters of Isfahan Metro Line 1, the train movement graphs and train timetables are extracted. Because the results obtained in the mechanical simulator section are used as necessary input for the electrical simulator program of the electric railway line.

Table 3: Location of Passenger Stations and Traction Substations in The Up Track of Isfahan Metro Line 1

Station Code	Passenger Station Name	Position (m)	Traction Substation	
1	GHO	Ghods	0	TSS1
2	BAHA	Baharestan	1380	-
3	GOL	Golestan	2780	-
4	MOF	Shahid Mofateh	4106	TSS2
5	ALI	Shahid Alikhani	5404	-
6	JAB	Jaber	6538	-
7	KAV	Kaveh	7833	TSS3
8	CHA	Shahid Chamran	9131	-
9	BAHO	Shahid Bahonar	10037	-
10	SHO	Meydan Shohada	10873	TSS4
11	TAK	Takhti	11748	-
12	EMH	Emam Hossein	12472	-
13	ENG	Enghelab	13482	-
14	33POL	Si-o-se-pol	14599	TSS5
15	MIR	MIR	15056	-
16	SHA	Doctor Shariati	15748	-
17	AZA	Azadi	16467	-
18	DAN	Daneshgah	17312	TSS6
19	KAR	Kargar	18409	-
20	KUE	Kuy-e-Emam	19279	-
21	DEMO	Defa-e- Moghadas	20464	TSS7

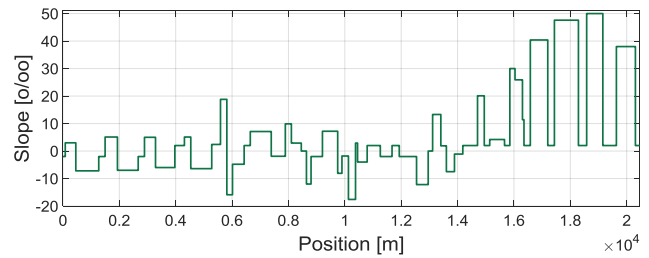


Fig. 5: The gradient profile of Isfahan Metro Line 1 for the up track.

According to the mechanical and dynamic equations of train movement that were introduced in section 2 and also using the route parameters of Isfahan Metro Line 1, the train movement graphs and train timetables are extracted. Because the results obtained in the mechanical simulator section are used as necessary input for the electrical simulator program of the electric railway line. In Fig. 6, the speed-distance profile of the first train of Isfahan Metro Line 1 is represented for the up direction. Furthermore, the speed limit of the train on the route is presented by the red dashed line. In Fig. 7, the distance-time graph of the first train of Isfahan Metro Line 1 is represented for the up direction. In Fig. 8, the timetable graph is presented for 14 trains on each track. A 2.5 min headway and a 1 min dwell time is considered. By using the train movement graphs, the electric power graphs of the trains are extracted in the double-track railway line. Fig. 9 shows the power demand-distance profile of the first train of Isfahan Metro Line 1 is represented for the up and down directions.

The electrical simulator program for train movement in both directions of Isfahan Metro Line 1 is obtained by Matlab software. For power flow analysis, the simulation time step has been considered 5 sec. The simulation results of a moving train on Isfahan Metro Line 1 are presented for both movement directions. In this program, the voltage and current values in the electric railway network are obtained by using the train timetable and the electric power curves.

The simulation results of the dc electric metro system for a moving train with regenerative braking are shown in Figs. 10-11. It is assumed that all traction substations can return the braking energy to the power grid. Therefore, in braking conditions, the braking energy of the train is used to provide the power of the auxiliary equipment, and its surplus is returned to the power grid.

In Fig. 10(a), the actual train power waveform, the pantograph voltage, and the train current are shown during the train movement from the GHO to the DEMO stations taking into account the regenerative braking. In Fig. 10(b), the actual train power waveform, the pantograph voltage, and the train current are shown during the train movement from the DEMO to the GHO stations taking into account the regenerative braking.

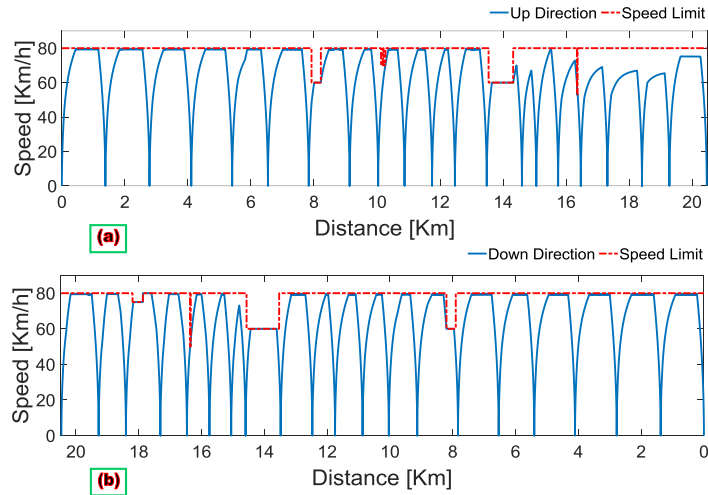


Fig. 6: The speed-distance profile of Isfahan Metro Line 1 for: a) up direction, b) down direction.

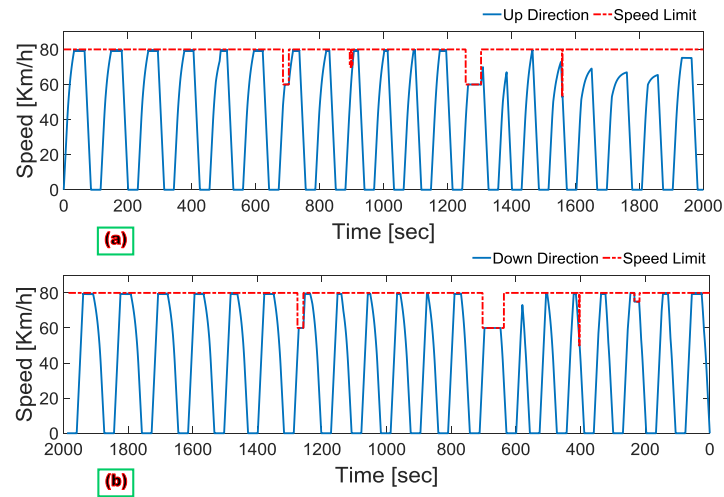


Fig. 7: The speed-time graph of Isfahan Metro Line 1 for: a) up direction, b) down direction.

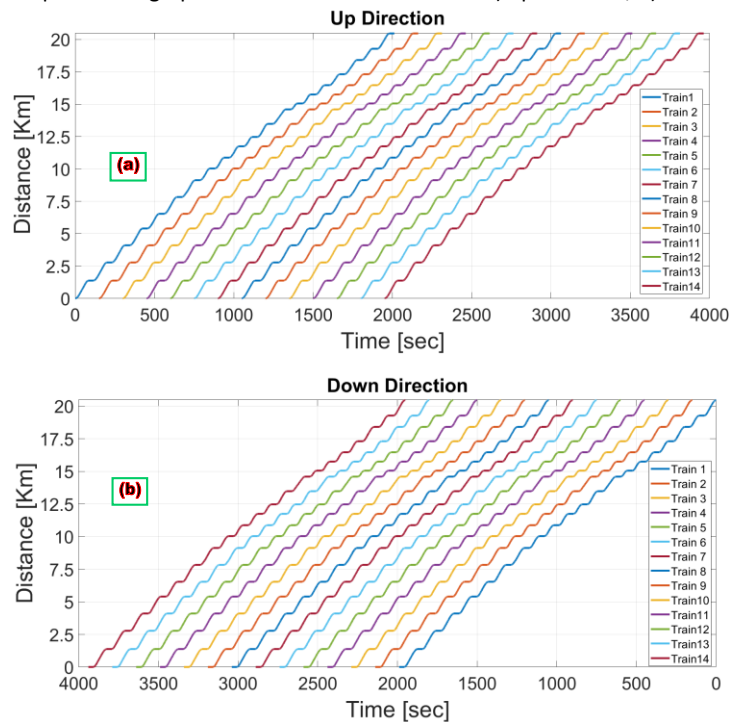


Fig. 8: The timetable graph of Isfahan Metro Line 1 for: a) up direction, b) down direction.

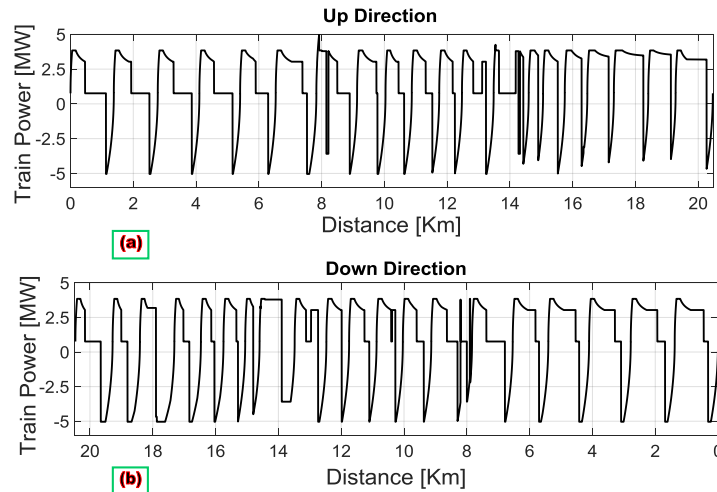


Fig. 9: The power demand-distance profile of Isfahan Metro Line 1 for: a) up direction, b) down direction.

As it is obvious, the train current is consistent with the electric power demand of the train, which shows the correctness of the power flow. But the pantograph voltage has an opposite relationship with its electric power demand. In this way, at the time of maximum power absorption from the electrical network, due to the increase in the current of the overhead network, the pantograph voltage drops and is at its minimum value. Also, in braking times, the excess power of the train is injected into the electrical network, and thus, overvoltage and undervoltage occur in the overhead contact line and the substation busbar. Therefore, at the maximum braking power of the train, the pantograph voltage

reaches its maximum. The obtained results show the correctness of the electric power flow program of the train

In Fig. 11, the voltage waveform of the traction substations is shown during the train movement from the GHO station to the DEMO station taking into account the regenerative braking. As it is clear, with the train movement on the railway track, the voltage of the busbar connected to the traction substation fluctuates. The highest amount of fluctuation is related to the substation that is closest to the train. As the train moves away from the traction substations, the voltage fluctuations decrease and vice versa.

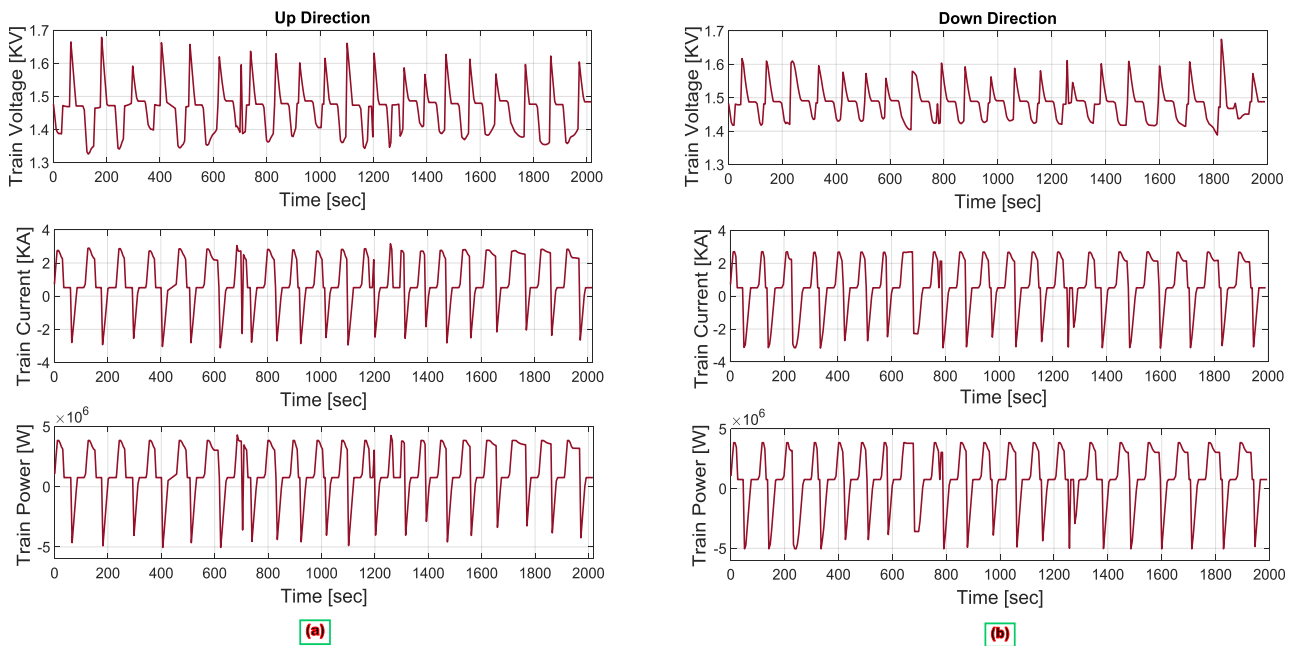


Fig. 10: The pantograph voltage, the pantograph current, and the train power demand during a single train movement on: a) up track, b) down track.

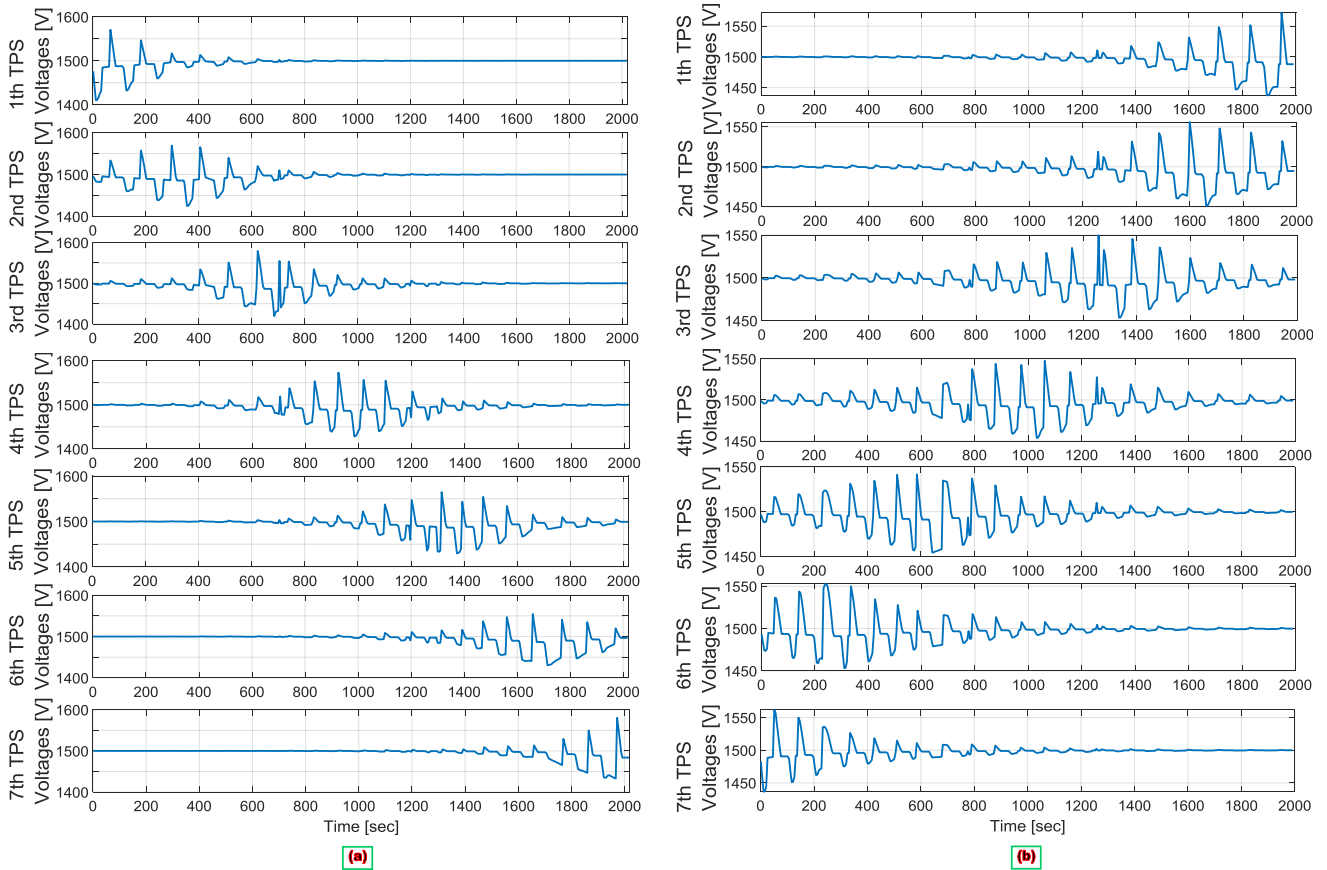


Fig. 11: The substations' voltages during a single train movement on: a) up track, b) down track.

Conclusion

The principal purpose of this paper is to suggest a DC electric railway network simulator including the train movement and traction power network. Simulation results based on the Isfahan Metro line are illustrated. Train current, voltage, and power assessment results manifest the simplicity and effectiveness of the proposed method for planning and operation investigations. The simulator can provide train current and voltage at any position in the track and additionally, the substation voltages by the train movement. The proposed model contains driving control modes with coasting control. Furthermore, the model includes regenerative braking on trains that cause overvoltage in the feeding line and substation busbars. The future work will focus on developing a multi-train simulator for the DC electric railway system including detailed energy consumption evaluation. Furthermore, over-voltage and under-voltage control strategies as well as rail potential assessment will be investigated.

Author Contributions

All authors contributed to the study conception and interpretation of results. P. Hamedani carried out the simulation results, wrote the manuscript, and supervised the project.

Acknowledgment

This work has been supported by the Center for International Scientific Studies & Collaborations (CISSC), Ministry of Science, Research, and Technology of Iran.

The authors gratefully acknowledge the Isfahan Regional Metro Company for providing the simulation parameters of Line 1.

Conflict of Interest

The authors declare no potential conflict of interest regarding the publication of this work. In addition, the ethical issues including plagiarism, informed consent, misconduct, data fabrication and, or falsification, double publication and, or submission, and redundancy have been completely witnessed by the authors.

Abbreviations

<i>OCL</i>	Overhead Contact Line
<i>OCS</i>	Overhead Contact System
<i>RCR</i>	Return Current Circuit

References

- [1] M. Brenna, F. Foiadelli, D. Zaninelli, *Electrical Railway Transportation Systems*, Wiley-IEEE Press, 2018.
- [2] A. A. Mohamed, A. Arshan Khan, A. T. Elsayed, M. A. Elshaer, *Transportation Electrification: Breakthroughs in Electrified*

- Vehicles, Aircraft, Rolling Stock, and Watercraft, Wiley-IEEE Press, 2023.
- [3] T. Fella, C. J. Goodman, P. Weston, (2010), "Validation of multi train simulation software," presented at the IET Conference on Railway Traction Systems (RTS), 2010.
- [4] T. Kulworawanichpong, "Multi-train modeling and simulation integrated with traction power supply solver using simplified Newton–Raphson method," *J. Mod. Transport*, 23: 241-251, 2015.
- [5] M. Chymera, C. J. Goodman, "The calculation of train performance," in *Proc. IET 13th Professional Development Course on Electric Traction Systems*: 1-13, 2014.
- [6] Z. Wu, C. Gao, T. Tang, "An optimal train speed profile planning method for induction motor traction system," *Energies*, 14(16): 5153, 2021.
- [7] D. Hu, Y. Yan, Z. Li, "Optimization methodology for coasting operating point of high-speed train for reducing power consumption," *J. Cleaner Prod.*, 212: 438-446, 2019.
- [8] Y. Arikan, E. Çam, "Optimizing of speed profile in electrical trains for energy saving with dynamic programming," presented at the International Symposium on Multidisciplinary Studies and Innovative Technologies, 2019.
- [9] N. Zhao, C. Roberts, S. Hillmansen, Z. Tian, P. Weston, L. Chen, "An integrated metro operation optimization to minimize energy consumption," *Transp. Res. Part C*, 75: 168-182, 2017.
- [10] Q. Lai, J. Liu, A. Haghani, L. Meng, Y. Wang, "Energy-efficient speed profile optimization for medium-speed maglev trains," *Transp. Res. Part E Logist. Transp. Rev.*, 141, 2020.
- [11] P. Martínez Fernández, I. Villalba Sanchís, V. Yepes, R. Insa Franco, "A review of modelling and optimisation methods applied to railways energy consumption," *J. Cleaner Producti.*, 222: 153-162, 2019.
- [12] L. Yang, K. Li, Z. Gao, X. Li, "Optimizing trains movement on a railway network," *Omega*, 40(50): 619-633, 2012.
- [13] V. Martinisa, M. Gallob, "Models and methods to optimize train speed profiles with and without energy recovery systems: A suburban test case," *Procedia Social Behav. Sci.*, 87: 222-233, 2013.
- [14] K. Bih-Yuan, L. Jen-Sen, "Solution of DC power flow for nongrounded traction systems using chain-rule reduction of ladder circuit Jacobian matrices," *ASME/IEEE Jt Railr Conf.*, 2002.
- [15] T. Yii-Shen, W. Ruay-Nan, C. Nanming, "Electric network solutions of DC transit systems with inverting substations," *IEEE Trans. Veh. Technol.*, 47(4): 1405-1412, 1998.
- [16] C. T. Tse, K.L. Chan, S. L. Ho, S. C. Chow, W. Y. Lo, "Tracking techniques for DC traction loadflow," in *Proc. International Conference on Developments in Mass Transit Systems*: 286-290, 1998.
- [17] T. Kulworawanichpong, "Simplified Newton–Raphson power-flow solution method", *Int. J. Electr. Power Energy Syst.*, 32(6): 551-558, 2010.
- [18] H. Alnuman, D. Gladwin, M. Foster, "Electrical modelling of a DC railway system with multiple trains," *Energies*, 11(11): 3211, 2018.
- [19] Z. Tian, S. Hillmansen, C. Roberts, P. Weston, N. Zhao, L. Chen, M. Chen, "Energy evaluation of the power network of a DC railway system with regenerating trains," *IET Electr. Syst. Transp.*, 6(2): 41-49, 2016.
- [20] C. L. Pires, S. I. Nabeta, J. R. Cardoso, "ICCG method applied to solve DC traction load flow including earthing models," *IET Electr. Power Appl.*, 1(2): 193-198, 2007.
- [21] Y. Cai, M. R. Irving, S. H. Case, "Iterative techniques for the solution of complex DC-rail-traction systems including regenerative braking," *IEE Proc. Gener. Transm. Distrib.*, 142(5): 445-452, 1995.
- [22] Y. Cai, M.R. Irving, S.H. Case, "Modelling and numerical solution of multibranch DC rail traction power systems," *IEE Proc., Electr. Power Appl.*, 142(5): 323-328, 1995.
- [23] R. A. Jabr, I. Džafić, "Solution of DC railway traction power flow systems including limited network receptivity," *IEEE Trans. Power Sys.*, 33(1): 962-969, 2018.
- [24] M. Popescu, A. Bitoleanu, "A review of the energy efficiency improvement in DC railway systems," *Energies*, 12: 1092, 2019.
- [25] Z. Tian, P. Weston, N. Zhao, S. Hillmansen, C. Roberts, L. Chen, M. Chen, "System energy optimisation strategies for metros with regeneration," *Transp. Res. Part C Emerg. Technol.*, 75: 120-135, 2017.
- [26] S. Lin, D. Huang, A. Wang, Y. Huang, L. Zhao, R. Luo, G. Lu, "Research on the regeneration braking energy feedback system of urban rail transit," *IEEE Trans. Veh. Technol.*, 68(8): 7329-7339, 2019.
- [27] M. Davoodi, H. Jafari Kaleybar, M. Brenna, D. Zaninelli, "Energy management systems for smart electric railway networks: A methodological review," *Sustainability*, 15(16): 12204, 2023.
- [28] X. Shen, H. Wei, T. T. Lie, "Management and Utilization of Urban Rail Transit Regenerative Braking Energy Based on the Bypass DC Loop," *IEEE Trans. Transp. Electrifi.*, 7(3): 1699-1711, 2021.
- [29] S. Park, S.R. Salkuti, "Optimal energy management of railroad electrical systems with renewable energy and energy storage systems," *Sustainability*, 11(22): 6293, 2019.
- [30] F. Lin, S. Liu, Z. Yang, Y. Zhao, Z. Yang, H. Sun, "Multi-Train energy saving for maximum usage of regenerative energy by dwell time optimization in urban rail transit using genetic algorithm," *Energies*, 9(3): 208, 2016.
- [31] Z. Tian, N. Zhao, S. Hillmansen, S. Su, C. Wen, "Traction power substation load analysis with various train operating styles and substation fault modes," *Energies*, 13(11): 2788, 2020.
- [32] Z. Tian, "System energy optimisation strategies for DC railway traction power networks," Ph.D. dissertation, Dept. of Electronic, Electrical and Systems Eng., University of Birmingham, UK, 2017.

Biographies



Pegah Hamedani was born in Isfahan, Iran, in 1985. She received B.Sc. and M.Sc. degrees from University of Isfahan, Iran, in 2007 and 2009, respectively, and the Ph.D. degree from Iran University of Science and Technology, Tehran, in 2016, all in Electrical Engineering. Her research interests include power electronics, control of electrical motor drives, supply system of the electric railway (AC and DC), linear motors & MAGLEVs, and analysis of overhead contact systems. She is currently an Assistant Professor with the Department of Railway Engineering and Transportation Planning, University of Isfahan, Isfahan, Iran. Dr. Hamedani was the recipient of the IEEE 11th Power Electronics, Drive Systems, and Technologies Conference (PEDSTC'20) best paper award in 2020.

- Email: p.hamedani@eng.ui.ac.ir
- ORCID: [0000-0002-5456-1255](https://orcid.org/0000-0002-5456-1255)
- Web of Science Researcher ID: AAN-2662-2021
- Scopus Author ID: 37118674000
- Homepage: <https://engold.ui.ac.ir/~p.hamedani/>



Seyed Saeed Fazel was born in Iran, in 1966. He received the M.Sc. degree in Electrical Engineering from the Iran University of Science and Technology, Tehran, Iran, in 1993, and the Ph.D. degree in Electrical Engineering from the Berlin University of Technology, Germany, in 2007. He spent four years (1994–1998) as an Engineer with Jihad Daneshgahi Elm Va Sanat (JDEVS). Since 1998, he has been an Assistant Professor with the Iran University of Science

and Technology. His research interests include power electronics, medium voltage converter topologies, and electrical machines.

- Email: fazel@iust.ac.ir
- ORCID: [0000-0002-7220-0146](https://orcid.org/0000-0002-7220-0146)
- Web of Science Researcher ID: NA
- Scopus Author ID: NA
- Homepage: <http://www.iust.ac.ir/content/3123/Dr.fazel>



Mahmoud Shahbazi received the B.Sc. degree in electrical engineering from the Isfahan University of Technology, Isfahan, Iran, in 2005, the M.Sc. degree in Electrical Engineering from the Amirkabir University of Technology, Tehran, Iran, in 2007, and the Ph.D. degrees in Electrical Engineering from the Université de Lorraine, Nancy, France and the Sharif University of Technology, Tehran, Iran, in 2012. He is currently an Associate

Professor in Electrical Engineering with the Department of Engineering, Durham University, Durham, U.K. His research interests include renewable energy integration, microgrids, power electronic converters and health monitoring, and fault-tolerant operation in these systems.

- Email: mahmoud.shahbazi@durham.ac.uk
- ORCID: [0000-0002-6057-3228](https://orcid.org/0000-0002-6057-3228)
- Web of Science Researcher ID: NA
- Scopus Author ID: 37091679200
- Homepage: <https://www.durham.ac.uk/staff/mahmoud-shahbazi/>

How to cite this paper:

P. Hamedani, S. S. Fazel, M. Shahbazi, “Modeling and simulation of DC electric railway system with regenerative braking: A case study of isfahan metro line 1,” *J. Electr. Comput. Eng. Innovations*, 12(2): 439-448, 2024.

DOI: [10.22061/jecei.2024.10665.728](https://doi.org/10.22061/jecei.2024.10665.728)

URL: https://jecei.sru.ac.ir/article_2098.html

